

RESEARCH ARTICLE

10.1002/2013JD021161

Key Points:

- Total precipitation amount does not have any trend in Northern China
- Rainfall trends differ between mountain and plains
- The trend contrast echoes aerosol effects

Correspondence to:

Z. Li,
zli@atmos.umd.edu

Citation:

Guo, J., M. Deng, J. Fan, Z. Li, Q. Chen, P. Zhai, Z. Dai, and X. Li (2014), Precipitation and air pollution at mountain and plain stations in northern China: Insights gained from observations and modeling, *J. Geophys. Res. Atmos.*, 119, doi:10.1002/2013JD021161.

Received 15 NOV 2013

Accepted 25 MAR 2014

Accepted article online 30 MAR 2014

Precipitation and air pollution at mountain and plain stations in northern China: Insights gained from observations and modeling

Jianping Guo^{1,2}, Minjun Deng¹, Jiwen Fan³, Zhanqing Li^{2,4}, Qian Chen⁵, Panmao Zhai¹, Zhijian Dai⁶, and Xiaowen Li⁷

¹Institute of Atmospheric Composition, Chinese Academy of Meteorological Sciences, Beijing, China, ²Department of Atmospheric and Oceanic Sciences and Earth System Science Interdisciplinary Center, University of Maryland, College Park, Maryland, USA, ³Atmospheric Science and Global Change Division, Pacific Northwest National Laboratory, Richland, Washington, USA, ⁴College of Global Change and Earth System Sciences, Beijing Normal University, Beijing, China, ⁵Nanjing University of Information Science and Technology, Nanjing, Jiangsu, China, ⁶Meteorological Institute of Jiangxi Meteorological Bureau, Nanchang, Jiangxi, China, ⁷School of Geography, Beijing Normal University, Beijing, China

Abstract We analyzed 40 year data sets of daily average visibility (a proxy for surface aerosol concentration) and hourly precipitation at seven weather stations, including three stations located on the Taihang Mountains, during the summertime in northern China. There was no significant trend in summertime total precipitation at almost all stations. However, light rain decreased, whereas heavy rain increased as visibility decreased over the period studied. The decrease in light rain was seen in both orographic-forced shallow clouds and mesoscale stratiform clouds. The consistent trends in observed changes in visibility, precipitation, and orographic factor appear to be a testimony to the effects of aerosols. The potential impact of large-scale environmental factors, such as precipitable water, convective available potential energy, and vertical wind shear, on precipitation was investigated. No direct links were found. To validate our observational hypothesis about aerosol effects, Weather Research and Forecasting model simulations with spectral-bin microphysics at the cloud-resolving scale were conducted. Model results confirmed the role of aerosol indirect effects in reducing the light rain amount and frequency in the mountainous area for both orographic-forced shallow clouds and mesoscale stratiform clouds and in eliciting a different response in the neighboring plains. The opposite response of light rain to the increase in pollution when there is no terrain included in the model suggests that orography is likely a significant factor contributing to the opposite trends in light rain seen in mountainous and plain areas.

1. Introduction

An increase in the concentration of submicron aerosol particles, which serve as cloud condensation nuclei (CCN), generally leads to an increase in the cloud droplet number concentration and a reduced cloud droplet effective radius [Twomey, 1977]. This process suppresses coalescence and collision into raindrops and thereby delays the growth of droplets and prolongs cloud lifetimes for warm clouds [Albrecht, 1989]. For deep mixed-phase clouds, delayed warm-rain processes could lead to the freezing of a greater amount of cloud water lifted above the freezing level, which could fuel the growth into deep convective clouds. This would substantially change the precipitation regime [Li et al., 2011a; Rosenfeld et al., 2008b], which remains not well understood yet. Aerosol particles such as dust may serve as effective ice nuclei to enhance ice crystal formation and increase snow precipitation in orographic clouds below 0°C [Fan et al., 2013; Niemand et al., 2012].

For convective clouds, observations and model analyses have reported both enhanced [Koren et al., 2012; Lin et al., 2006; Zhang et al., 2007] and suppressed [Givati and Rosenfeld, 2004; Jiang et al., 2008; Rosenfeld, 1999] precipitation by aerosols, depending on environmental conditions [Khain, 2009; Fan et al., 2009; Tao et al., 2007]. The overall effect of aerosols on precipitation depends on the dynamic balance between condensate generation (droplet condensation and ice deposition) and condensate loss (evaporation and sublimation), which can be modified by factors such as cloud type, air humidity, and wind shear [Khain, 2009]. In addition, aerosol effects on precipitation have an opposite effect when the aerosol concentration is greater than an optimal value [Koren et al., 2008; Rosenfeld et al., 2008b]. The buffering mechanism that exists in aerosol-cloud-precipitation systems may make the estimation of the precipitation response to an aerosol perturbation especially daunting and even controversial [Stevens and Feingold, 2009]. This demonstrates the

necessity of further investigating aerosol indirect effects on precipitation through a combination of in situ observations and model simulations.

Due to rapid economic development over the past few decades, China has become a major source of anthropogenic aerosol particles in the world [Li *et al.*, 2007, 2011b; Qian *et al.*, 2006]. These aerosols have a serious impact on air quality and climate [Feingold *et al.*, 2005]. Analyzing half a century of meteorological data, Qian *et al.* [2009] found that the precipitation pattern in China has undergone a drastic change with a decreasing frequency of light rain, but increasing frequency of heavy rain, which was argued to be caused by increasing aerosol loading in the region.

Due to the exceptionally high proportion of energy generated from coal burning, the black carbon (BC), or soot, concentration is high over parts of China. Using a combination of satellite and surface measurements, Lee *et al.* [2007] derived the distribution of the single-scattering albedo (SSA) across China. The lowest SSA is found in northeast and central China, while the highest SSA is found in southeast (SE) China. Analyzing long-term surface and satellite data of thunderstorms, opposite trends were found: a decrease in the number of thunderstorms over central China [Yang *et al.*, 2013a] and an increase in the number of thunderstorms over SE China [Yang and Li, 2014] and south China [Wang *et al.*, 2011]. This suggests two different effects due to two distinct types of aerosols: radiative heating by BC and the invigoration effect by sulfate aerosols which tends to suppress and enhance convection, respectively. Atmospheric heating and surface cooling by BC results in a more stable atmosphere and thus suppresses convection and precipitation. This effect was simulated by models over China [Wu *et al.*, 2013; Zhang *et al.*, 2012] and falls within the broad framework proposed by Wang *et al.* [2013]. However, evidence presented thus far has been circumstantial and awaits affirmation from different perspectives and in different regions/seasons affected by different types of aerosols. A unique perspective is to make use of topography [Alpert *et al.*, 2008; Houze, 2012]. Due to topographic forcing, air in front of a mountain is lifted and produces more rainfall than in the upwind plains. The ratio of annual precipitation amount at a mountain station to that at a nearby upwind plain station, called the topographic enhancement factor (R_o), tends to be reduced by aerosols because it leads to small cloud droplets and thus decreases precipitation, as demonstrated by Rosenfeld *et al.* [2007] using long-term meteorological rainfall data from Hua Mountain and a nearby plain station in central China. By virtue of such a contrast between mountain and plain stations, Yang *et al.* [2013a, 2013b] extended the study to single out noticeable effects of aerosols on almost all meteorological variables (temperature, wind, precipitation, thunderstorms, etc.) in central and SE China.

The North China Plain (NCP, a typical plain region) is a highly urbanized area where a severe degradation in air quality has occurred in recent years [Guo *et al.*, 2011]. The dominant role of urban pollution on precipitation in downwind regions has been demonstrated [Carrió *et al.*, 2010; Halfon *et al.*, 2009; Russell and Hughes, 2012; van den Heever and Cotton, 2007]. The Taihang mountain range (hereafter called Taihang) is located downwind of urban areas under the influence of the Asian summer monsoon. The goal of the study is to examine changes in precipitation caused by topographically produced clouds and to evaluate how air pollution from the urban area, which is mainly composed of anthropogenic emissions, affects the downwind mountainous area. To further verify our hypothesis about the impact of aerosols, we conduct cloud-resolving model simulations using the Weather Research and Forecasting (WRF) model coupled with spectrum-bin microphysics (SBM) [Fan *et al.*, 2012a; Khain *et al.*, 2004] for a case study over the study region.

Section 2 describes data sets used in this study, as well as model experiments performed and the general methodology used. Trends in total rainfall amount and in different precipitation categories, as well as modeling results from two sensitivity experiments using clean and polluted conditions are presented in section 3. Conclusions are drawn in section 4.

2. Data and Methods

2.1. The Study Region

Taihang is a major mountain range in northern China, stretching more than 400 km from north to south. To the east lies the NCP, which is one of the main hubs of China's economic growth and one of the most densely urbanized regions in the world. It includes metropolises like Beijing, Tianjin, Shijiazhuang, and Baoding. Figure 1a shows the locations of the NCP and the seven rain gauge stations selected for the study (see Table 1). Of the seven stations, four are located in urbanized areas in the plains while the remaining three

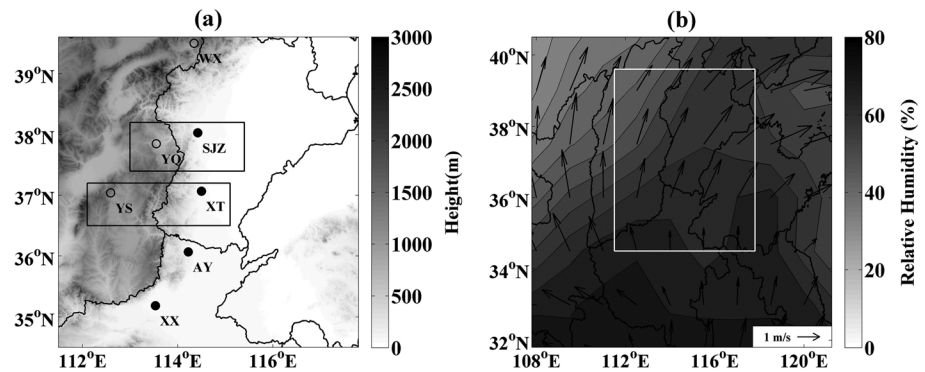


Figure 1. (a) Locations of the North China Plain (NCP) and the seven rain gauge stations selected for study (solid dots), where the shaded background shows the terrain elevation. The two-way nested domains (1 and 2) have a horizontal grid spacing of 12 km and 2.4 km, respectively. (b) White rectangle inserted indicates domain 2, namely the spatial range shown in Figure 1a. Domain 1 represents the spatial range in Figure 1b. Three (four) mountainous (plain) rain gauge stations are shown in open (solid) dots and “mountain-plain” pairs of stations used for further analysis are enclosed within rectangles in Figure 1a. Figure 1b is a composite of mean 850 hPa vector wind and relative humidity fields on the basis of ERA-Interim reanalysis data during the summertime seasons of 1979–2005.

stations are distributed across Taihang and are downwind of the urban areas during the summer. Precipitation at the mountain stations is presumably affected by both air pollution and orography. All stations have long-term records of meteorological data. Our study is based on long-term measurements of visibility reported every 3 h and hourly precipitation measurements made at these stations during the summer seasons of 1966–2005.

Figure 1b shows mean 850 hPa vector wind and relative humidity (RH) fields from the latest European Centre for Medium-Range Weather Forecasts global atmospheric reanalysis (ERA-Interim) [Dee et al., 2011] data over the study area during the summers of 1966–2005. Based on RH and prevailing winds, two pairs of sites are chosen: SJZ/YQ and YS/XT (outlined by rectangles in Figure 1b). RH conditions at the locations of each pair are similar, and the mountain sites (YQ and YS) are located downwind of the plain sites (SJZ and XT) influenced by the prevailing southeastern monsoon circulation. The distance between YQ and SJZ (YS and XT) is about 80 km (170 km). The elevation difference between YQ and SJZ (YS and XT) is roughly 600 m (900 m). These two pairs of sites are singled out for further analysis regarding the decoupling of aerosol and orographic effects in the long-term precipitation signal.

2.2. Observational Data

Visibility has been widely used as a surrogate for aerosols to characterize the ambient environment and to study the impact of aerosols on precipitation even though it has large uncertainties [Hand et al., 2002; Qian et al., 2009; Rosenfeld et al., 2007]. For the sake of long-term trend analyses, visibility is used because it has a much longer record [Che et al., 2007] than other more direct measurements of environmental quantities, e.g., particulate matter and aerosol optical depth. Measuring the latter is a more recent scientific activity, and these measurements have varying accuracies [Xin et al., 2007]. Long-term hourly precipitation and daily horizontal visibility data sets, covering the period of 1966 to 2005 at more than 200 stations distributed

Table 1. Description of the Seven Weather Stations Selected for Analysis

Station Name	Latitude (°)	Longitude (°)	Altitude (m)	Geographic Location
Xinxiang (XX)	35.19	113.53	74	south of Taihang
Anyang (AY)	36.07	114.22	76	southeast of Taihang
Yushe (YS)	37.07	112.98	1042	in Taihang
Xingtai (XT)	37.07	114.50	78	east of Taihang
Yangquan (YQ)	37.85	113.55	743	in Taihang
Shijiazhuang(SJZ)	38.03	114.42	81	east of Taihang
Weixian (WX)	39.50	114.34	910	in Taihang

throughout China, have been quality-controlled and archived by the National Meteorological Information Center. Horizontal visibility measurements collected during nonfoggy and nonprecipitation days are selected to ensure that only aerosols are the cause for any diminishment of visibility at a given station. Surface winds and cloud-base heights measured at four local solar times (LST; 02, 08, 14, and 20 LST) are also used. Tests for anomalous values and data continuity have been performed on all meteorological data. The summer period (May, June, July, August, and September; MJJAS) has been chosen for analysis because it is the major rainy season at most stations in the NCP and the adjacent Taihang.

Atmospheric data used in this study are from ERA-Interim reanalysis data set, including, among others, temperature, vorticity, wind vectors, and humidity at 37 pressure levels ranging from 1000 hPa to 1 hPa. ERA-Interim data currently available are from January 1979 to May 2013, and are archived at $1.5^\circ \times 1.5^\circ$ resolution. Monthly mean data are averaged from daily data. The horizontal wind is decomposed into zonal (U) and meridional (V) components.

2.3. Methodology

Visibility measurements made before 1980 were recorded in terms of class, of which 10 were defined. After 1980, visibility was recorded as distance in kilometers. If precipitation or fog occurred at any time during a particular day, the visibility data for that day is excluded. To remove the humidity influence on visibility, all visibility data have been corrected for RH when RH is between 40% and 99%. Following *Rosenfeld et al.* [2007], the correction formula is

$$VIS_{dry} = \frac{VIS_{measured}}{0.26 + 0.4285 \times \log_{10}(100 - RH)} \quad (1)$$

where the RH is expressed in percent.

Changes in precipitation are analyzed for different levels of rain intensity over the period of 1966–2005. It is useful to study trends in different rain intensities, in addition to total rainfall, given their different roles in the hydrological cycle and in extreme events such as floods and droughts [*Goswami et al.*, 2006]. Similar to *Yum and Cha* [2010], rain intensity is classified into four categories: very low (VL; $\leq 0.6 \text{ mm h}^{-1}$), low (LO; $0.6\text{--}2 \text{ mm h}^{-1}$), moderate (MO; $2\text{--}8 \text{ mm h}^{-1}$), and high (HI; $> 8 \text{ mm h}^{-1}$).

Rain frequency is computed from hourly rainfall data, unlike many previous studies based on monthly or daily data [e.g., *Qian et al.*, 2009]. For each category of precipitation, the summertime occurrence frequency is calculated as the ratio of the total number of hours with rain in the category recorded during MJJAS divided by the total number of hours during the entire summertime ($153 \text{ days} \times 24 \text{ h/d}$). If the total number of hours of missing data exceeds 100, the year is excluded from the time series.

Sumner [1988] demonstrated that annual precipitation records at a single station have variations that are sometimes greater than the mean annual precipitation amount, leading to a coefficient of variation in excess of 100%. This results in statistical difficulties in estimating precipitation trends due to the asymmetry and the nonnormal distribution of annual precipitation measured over several decades at a single station [*Paldor*, 2008].

Aerosol-cloud-precipitation interaction mechanisms may be different for different precipitation types. It is highly likely that they might have different signs to offset each other when combined. Our study is focused on light rainfall to investigate any influential mechanisms. In general, two distinct mechanisms can contribute to long-term light rain changes. One is the light rain associated with the decaying stage, or stratiform portion, of a mesoscale system (MSS). The other is associated with weak orographic lifting, either by stratus or by small cumulus (ORO). The former mechanism is controlled strongly by synoptic-scale dynamics, and the latter mechanism is related more to the local instability. Consequently, the MSS light rain is counted as long as the following criteria are all met. (1) The rainfall belongs to long duration rainfall event; (2) There is at least one maximum hourly rainfall amount above a threshold (0.86 mm, i.e., the value corresponds to 65% of all the rainfall cases) of the summertime hourly rainfall event during 1965–2005. Regarding the ORO light rain, if the rainfall belongs to short-duration rainfall event and maximum hourly rainfall amount is 0.1 mm, then one ORO case is counted.

As proposed by *Yu et al.* [2007] and *Guo et al.* [2014], a short (long)-duration rainfall event that may be intermittent is defined here as rain falling for 1–2 h (more than 3 h) with no more than a total of 1 h of no rain

falling within the event. If the nonraining period lasts 2 h and subsequently, rain begins again, this is classified as a new rainfall event. Also, in the presence of NCP air pollution, we visually check whether there is any change in precipitation efficiency of orographic clouds (cf. section 3.3) at mountainous sites during the investigation period. Weather observations taken 4 times daily at each site were closely examined to determine if there were any orographic clouds present over the mountain station (YQ), and if at the same time, clear weather and easterly winds prevailed over the plain station (SJZ). If these preliminary conditions were met, the cloud-base height then had to be less than 1 km to minimize the impact of convective clouds. This cloudiness might also include fog or rain. These criteria are expected to ensure that YQ is downwind of SJZ and under the influence of orographic clouds.

Large-scale atmospheric conditions play important roles in precipitation. While numerous factors dictating the impact of aerosols on precipitation have been identified [Tao *et al.*, 2012], the two most widely recognized factors are water vapor and wind shear [e.g., Khain *et al.*, 2008]. As the first step in determining if key meteorological variables have experienced any long-term trends, we examine precipitable water (PW), or total column water vapor in the atmosphere, along with wind shear. Both PW and wind shear data sets are from the ERA-Interim reanalysis, PW is a significant factor that correlates well with precipitation [Zhai and Eskridge, 1997]. It can be derived by integrating specific humidity at various pressure levels starting from surface to the top of atmosphere (20 hPa) and is defined as follows

$$PW = \frac{1}{g} \int_{\text{surface}}^{10 \text{ hPa}} q dp \quad (2)$$

where g is the acceleration of gravity and q is the specific humidity. In this paper, for the mountainous area, there is a mean surface pressure of 925 hPa, whereas the plain area has a mean surface pressure of 1000 hPa, which is obtained from reanalysis data.

2.4. Model Experiments

To aid our understanding of the physical mechanisms governing aerosol-precipitation interactions over a mountainous environment, model simulations were conducted. Simulations have been performed using the WRF model version 3.2 coupled with the SBM [Fan *et al.*, 2012a, 2012b] based on the Hebrew University cloud model [Khain *et al.*, 2004]. The size distributions of hydrometeors and CCN are resolved by 33 mass doubling bins, i.e., the mass of particle m_k in the k th bin is determined as $m_k = 2 m_{k-1}$. Details about the version of SBM used in this study are described in many previous studies [Fan *et al.*, 2012a, 2012b; Khain, 2009; Khain *et al.*, 2010]. The Rapid Radiative Transfer Model for GCMs (RRTMG) shortwave and longwave radiation schemes are used with the effective radius calculated in the cloud microphysics module passed to the RRTMG radiation scheme.

A precipitation event that occurred over the Taihang mountain range and nearby plain regions on 13 July 2008, caused by the east-to-west passage of a cold front cloud system, is simulated. The system produced some shallow, stratiform, and deep clouds, and precipitation was widespread over the region. Clouds were mainly cold-based with cloud-base temperatures less than 8°C. Real-case simulations are performed with two-way nesting over two nested domains (Figure 1a) using the SBM scheme for both outer and inner domains. Simulations are run for 78 h (more than 3 days) with the first 6 h treated as a spin-up. Horizontal resolutions of 12 km and 2.4 km are used for the two nested domains; horizontal grid points for Domain 1 (coarse-grid domain) and Domain 2 (fine-grid domain) are 110×90 and 251×251 , respectively. National Centers for Environmental Prediction Final global reanalysis data on a $1^\circ \times 1^\circ$ grid for every 6 h are used to provide initial and boundary conditions. Simulations are performed on 41 vertical levels, with a stretched resolution in the range of 70–800 m from the lowest to the highest levels. To examine aerosol effects, two simulations were run by perturbing aerosols in both inner and outer domains from clean (CCN concentrations of 280 cm^{-3}) to polluted (CCN concentrations of $6 \times 280 \text{ cm}^{-3}$) conditions. Because of lacking reliable observations of CCN for the study region, we conducted these two simulations only for general clean and polluted clouds. Grids with altitude > 300 m and $10 \text{ m} < \text{altitude} < 100$ m in Domain 2 after excluding the boundary points (Figure 1a) are considered as mountainous and plain areas, respectively. Most rain gauges have a detection limit of 0.25 mm h^{-1} , so the threshold for a rainy grid is set to 0.25 mm h^{-1} to be consistent with observational analyses.

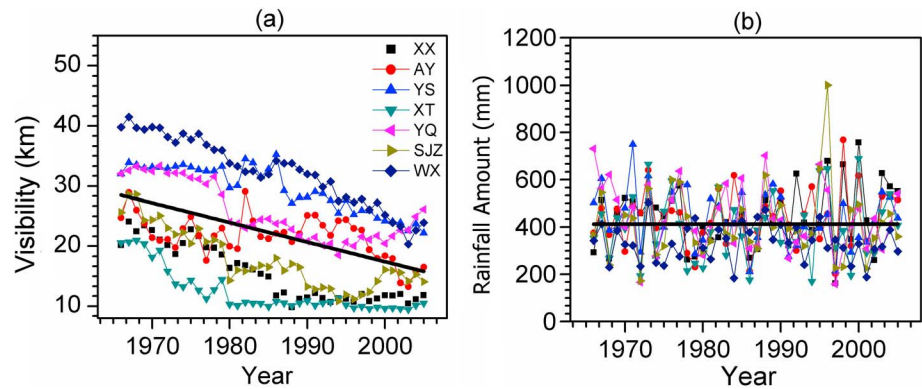


Figure 2. Time series of (a) summertime average visibility and (b) summertime total precipitation at the seven stations. Black lines represent mean trends.

3. Results and Discussion

3.1. Visibility and Total Precipitation Trends

Figure 2 shows time series of visibility and summertime precipitation from 1966 to 2005. Over the period of four decades, visibility has reduced by about half (14 km or 45%), suggesting deteriorating air quality in this region (Figure 2a). This decreasing trend coincides with an increasing trend in the number of aerosol particles due to anthropogenic emissions such as SO₂ [Gong *et al.*, 2007; Qian *et al.*, 2009]. This was extensively verified by Moderate Resolution Imaging Spectroradiometer aerosol optical depth retrievals [Guo *et al.*, 2011]. The greatest reduction in visibility (~18.8 km) is seen at the mountain station WX, presumably due to increasing pollution in the upstream urban area. There is no pronounced change in visibility at most stations after the year 2000, as more emission control measures were taken.

A very weak increase in precipitation amount (0.4 mm per decade) is seen over the period of 1995–2005 (Figure 2b). This is consistent with the broader trends observed in precipitation amount and frequency over northern China [Zhai *et al.*, 2005].

3.2. Variations and Trends in Different Precipitation Types

In light of the large year-to-year variation and no discernible change in summertime total precipitation amount over time at all stations (Figure 2b), the frequency of rainfall occurrence, as defined in section 2.3, was analyzed for the four categories of rainfall intensity (Table 2). All precipitation types at the mountain stations (except for the HI precipitation type at station WX) show a decreasing trend over the period of 1966–2005. The VL precipitation type shows the most pronounced reduction in terms of rainfall occurrence. At station YQ, for example, the number of hours with VL precipitation decreased by about 57% over the period of four decades. Trends are not consistent among the plain stations. All precipitation types at station XX show increasing trends of varying degree over the period of 1966–2005, but trends are less clear at other plain stations.

Table 2. Slopes and Pearson’s Correlation Coefficients for Trends in Variations of Summertime Occurrence Frequencies of Four Precipitation Categories During the Summer Seasons of 1966–2005

	XX	AY	SJZ	XT	YQ	YS	WX
Slope (unit: mm/yr)							
Very Low	0.38	0.14	-0.62	0.01	-0.57	-0.53	-0.51
Low	0.16	-0.08	-0.31	-0.28	-0.25	-0.29	-0.46
Moderate	0.15	-0.03	0.11	-0.06	-0.22	-0.46	-0.20
High	0.03	0.07	0.02	0.06	-0.05	-0.02	0.06
Correlation Coefficient							
Very Low	0.73	0.66	-0.21	0.21	-0.69	-0.68	-0.57
Low	0.69	-0.05	-0.20	-0.21	-0.45	-0.46	-0.59
Moderate	0.35	-0.03	0.08	-0.06	-0.47	-0.36	-0.20
High	0.27	0.18	0.06	0.13	-0.14	-0.04	0.21

^aNumbers in bold indicate statistical significance at the 5% confidence level.

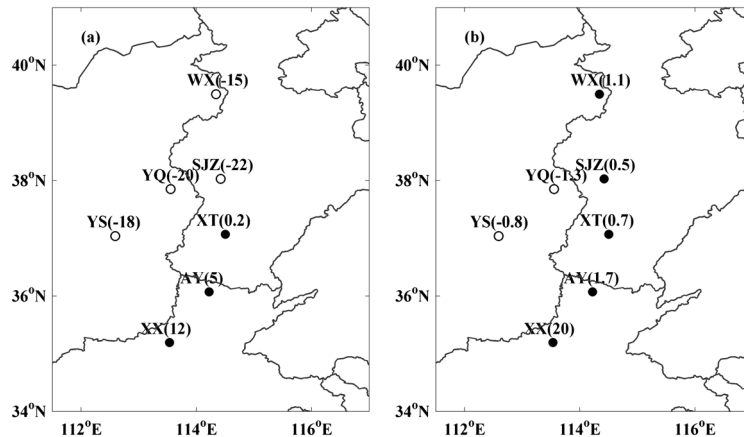


Figure 3. Trends (in percent) in variations of occurrence frequency for the (a) VL and (b) HI precipitation types during the period 1966–2005. The open circles indicate decreasing trend, and filled circles increasing trend. The significance test results were shown in Table 2.

Figure 3 shows trends in rainfall frequency for VL and HI precipitation types at the mountain and plain stations over the period of 1966–2005. Both light and heavy precipitation events have decreased at mountain stations, but light rain events have decreased much more drastically. At the plain stations, heavy rain events generally have an increasing trend, but this is not statistically significant, as shown in Table 2. This finding is consistent with results from studies focused on precipitation over western central China [Rosenfeld *et al.*, 2007; Yang *et al.*, 2013a]. They argued that the reduction in light rain was caused by increasing amounts of aerosols and that this was more significant over mountainous regions than over plain areas. As for heavy rain and storms, both observational and modeling studies have indicated that aerosols enhance such events under weak wind shear conditions [Fan *et al.*, 2012b, 2009; Li *et al.*, 2012], but this seems to be the case for plain stations and not for mountain sites. Storms over mountainous regions tend to have large wind shear due to the effects of terrain height and topography, which could lead to the reduced rain rate [Fan *et al.*, 2009]. Therefore, the decreased heavy rain frequency observed over mountainous regions may be explained by aerosol impacts. The intermediate precipitation types (LO and MO) are not as frequent as the VL and HI precipitation types, and their variations over the time period under study are not as distinct (not shown here).

3.3. Aerosol Effect on Orographic Precipitation

Orographic precipitation is reportedly more susceptible to aerosol pollution [Rosenfeld *et al.*, 2007; Yang *et al.*, 2013a, 2013b]. The physical mechanisms involved consist of a complex set of interactions between fluid dynamics, thermodynamics, and micron-scale cloud microphysical processes, as well as a dependence on the

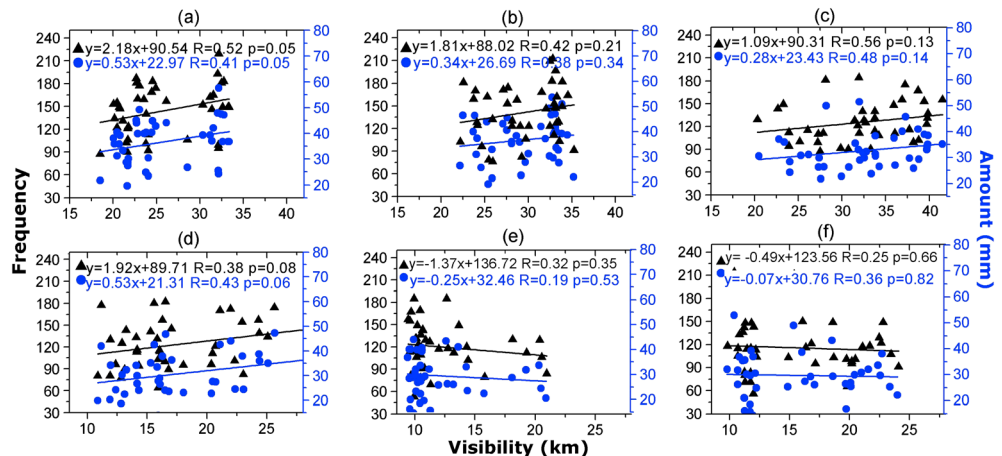


Figure 4. Summertime average light rain frequency/amount as a function of average visibility at stations (a) YQ, (b) WX, (c) SJZ, (e) XT, and (f) XX. Light rain refers to VL and LO precipitation types.

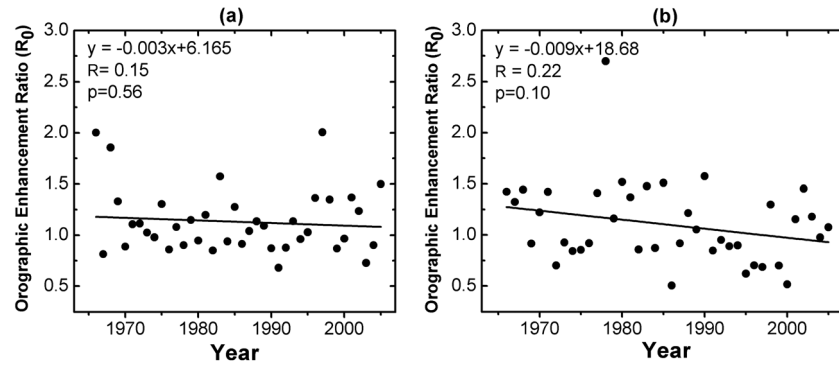


Figure 5. Time series of summertime average R_o for (a) the YQ/SJZ station pair and (b) the YS/XT station pair. Regression equations and correlation coefficients are shown in the left corner of each panel, and the p values from the F test for linear trend regression are reported as well.

atmospheric general circulation on a synoptic scale and the urban effect [Goldreich, 2003] at upwind plain stations. Long-lasting moderate-to-heavy rainfall occurs frequently when large-scale synoptic processes pass over the Taihang mountainous region, associated with the East Asia summer monsoon in northern China. Moderate and heavy precipitation events are largely controlled by synoptic weather systems, so it is very hard to separate the effect of aerosol particles from dynamic and thermodynamic factors. These events are excluded in the subsequent analysis.

Figure 4 shows the frequency of occurrence of light rain and rainfall amount as a function of visibility at six stations (plain station AY is not shown to simplify the graphical presentation). The number of light rain events and precipitation amount are positively correlated with visibility over mountain stations (Figures 4a–4c). No such consistent trends are seen at the four plain sites (except for SJZ). There is either a slight increase or decrease in the number of light rain events and precipitation amount with increasing visibility (Figures 4d–4f).

R_o [Givati and Rosenfeld, 2004; Rosenfeld et al., 2007] is used to overcome this inherently large variability in summertime precipitation at a single station. The time series of summertime average R_o from 1966 to 2005 at the two mountain–plain pairs of stations shown in Figure 2 is given in Figure 5. The summertime average total precipitation amount decreases over time at the two mountain stations. R_o for the YQ/SJZ and YS/XT pairs of mountain–plain stations decreased by 9% and 25%, respectively, suggesting a significant reduction in precipitation over the mountain regions as pollution upwind worsened over the years.

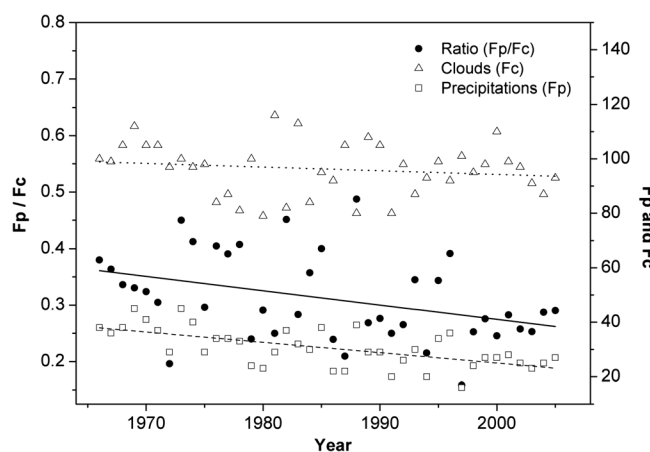


Figure 6. Time series of summertime occurrence frequencies of orographic clouds (Fc) and precipitation (Fp), and their ratio at the mountain station YQ. The ratio (Fp/Fc) acts as a proxy for the precipitation efficiency of orographic clouds. The trends in Fp/Fc (0.003 year⁻¹) and Fp (0.002 year⁻¹) are significant at the 0.05 confidence level in one sample t test.

Figure 5 reveals that R_o has decreased over time. Increasing air pollution in the NCP is likely one of the main factors responsible for the observed decreasing trends, especially for light rain over Taihang. When the atmosphere is pristine, the prevailing wind shown in Figure 1b would force a parcel of unsaturated air up and over Taihang, resulting in adiabatic expansion and eventual saturation. This would facilitate precipitation over the windward side of Taihang. As the upwind area of the mountain region becomes increasingly polluted, the prevailing wind would transport air pollution and aerosols toward the leeward side of Taihang. As a result of the increase in aerosol loading, the cloud droplet number would increase

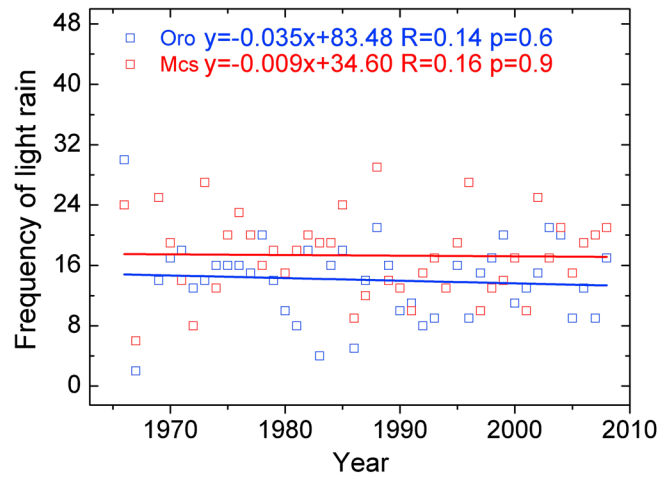


Figure 7. Temporal evolution of ORO (red open square) and MSS (blue open square) light rain occurrence frequency at Yangquan site during the period 1965–2005. Regression equations, correlation coefficients, and the p values from the F test for linear trend regression are reported as well.

while cloud droplet effective radii would decrease, resulting in a less efficient warm-rain process. This would slow down drizzle production and reduce the precipitation efficiency [Albrecht, 1989]. This scenario would explain the reduction in light rain events over Taihang.

Yum and Cha [2010] proposed a parameter called the precipitation efficiency of orographic clouds for better accounting for the suppression of light rain by air pollution. It is defined as the frequency of precipitation (F_p) divided by the frequency of orographic clouds (F_c). Light rain over mountain regions is mainly from clouds with weak convective strength, such as cumulus or stratiform clouds of shallow depth. Due to the lack of long-term

cloud observations for the XT/YS pair of weather stations, the following analysis is confined to the other pair of weather stations (SJZ and YQ). To single out the impact of aerosols, a subset of data was selected to ensure that the mountain site YQ was under the influence of orographic clouds and pollution from upper air winds. Requirements for the plain station (SJZ) are that the sky is cloud-free and that winds are easterly. Requirements for the mountain station (YQ) are that the sky is cloudy and that cloud bases are below 1 km above ground level. Visibilities at these two stations have a similar decreasing trend when winds are easterly. This helps strengthen the connection between pollution in the plain areas and precipitation over Taihang through the orographic effect.

Figure 6 shows time series of F_p , F_c , and F_p/F_c at station YQ. There is no significant variation in F_c , except for some high values during the 1980s. However, F_p has a significant decreasing trend. In turn, F_p/F_c decreases noticeably over time as well. The mean precipitation intensity from these orographic clouds is $0.67 \pm 0.32 \text{ mm h}^{-1}$, which is close to the upper limit of the VL precipitation type. If there is no systematic variation in the summertime frequency of occurrence of weakly convective clouds, the decrease in F_p/F_c over this mountainous region may serve as proof of the influence of air pollution on precipitation. This is verified by means of modeling with a cloud-resolving model as described below.

We also investigated light rain types and their variation trends in terms of formation mechanism (MSS and ORO). Figure 7 shows that both ORO and MSS light rain types have a decreasing trend during the study period. The ORO light rain type has a relatively steeper slope than the MSS light rain type, but both linear

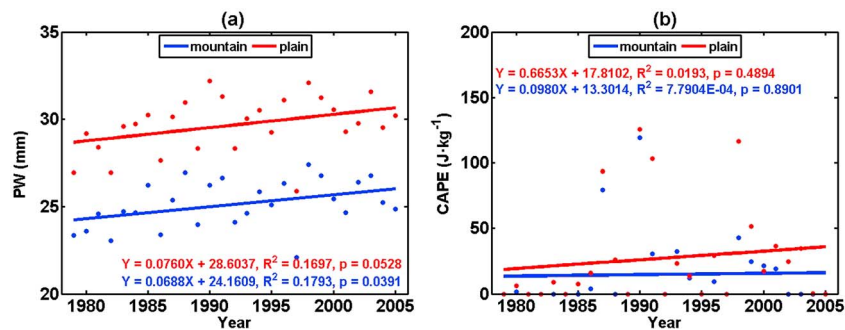


Figure 8. Time series of (a) precipitable water (PW) and (b) Convective Available Potential Energy (CAPE) over mountain (blue dots) and plain (red dots) areas during summertimes of the period 1979–2005. ERA-Interim data are used. Regression equations, correlation coefficients and the p values from the F test for linear trend regression are shown as well.

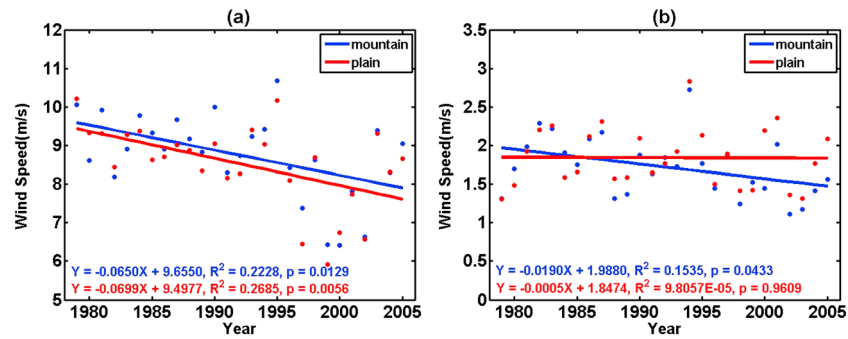


Figure 9. Time series of wind speed over mountain (blue dots) and plain (red dots) areas at (a) 500 hPa and (b) 800 hPa. ERA-Interim data from 1979–2005 are used. Regression equations, correlation coefficients and the p values from the F test for linear trend regression are shown as well.

regressions did not pass the significance test at the 5% confidence level. Therefore, we argue with high confidence that light rain has been suppressed at station YQ due to aerosol pollution in the NCP, irrespective of the light rain formation mechanism involved.

3.4. Trends in Atmospheric Environment Factors

The above inference may not be true if changes in meteorological factors could explain the aforementioned phenomena. Figure 8a shows long-term (1979–2005) trends in summertime mean PW over Taihang and the NCP. Qian *et al.* [2009] have conjectured that there may be a link between large-scale moisture in the atmosphere and light rain. Both mountainous and plain regions (defined in the same way as in the model experiment) show similar increasing trends even though the two regions have different light rain trends. So the decreasing trend in light rain observed over Taihang during the past three decades is not likely caused by changes in the large-scale moisture content. Moreover, atmospheric instability is one of the factors affecting convection initiation, thus changing the precipitation occurrence. The Convective Available Potential Energy (CAPE) exhibits an increasing trend in both mountainous and plain regions for the years investigated in this study, as shown in Figure 8b. This does not favor the suppression of light rain observed here. Figure 9 reveals long-term variations in wind speed over plain and mountain regions at 500 hPa and 800 hPa. Over Taihang, wind speed has decreased steadily at both levels over time. Wind speeds over the plains have changed little in the lower atmosphere but show a decreasing trend at 500 hPa. In general, aerosols originating from a land surface located at an altitude lower than a neighboring mountain cannot be easily transported to the midlevel atmosphere (500 hPa), so the decreasing wind at 500 hPa can only be attributed to changes in large-scale circulation rather than to aerosols. The 850 hPa level corresponds roughly to the surface level over most parts of Taihang. The weakening trend in wind speed over Taihang may be partly connected to the increase in aerosol pollution over the region.

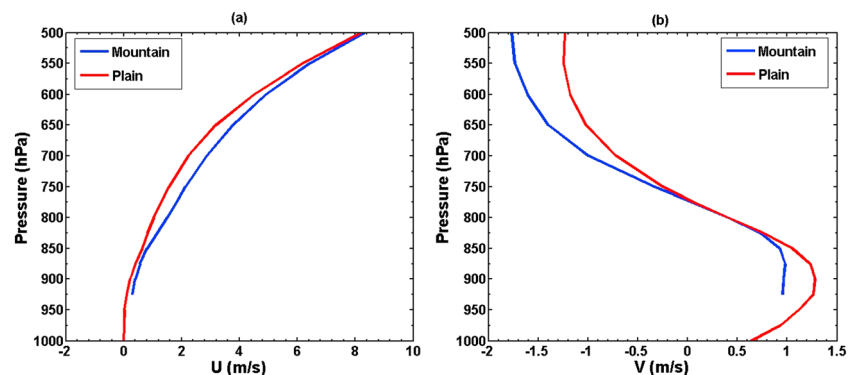


Figure 10. Profiles of mean (a) zonal (U) and (b) meridional (V) wind components over mountain (blue lines) and plain (red lines) areas during MJJAS of 1979–2005. Wind shear is calculated as $[\max(u)/\max(v)]$ minus $[\min(u)/\min(v)]$ within 5 km from the ground.

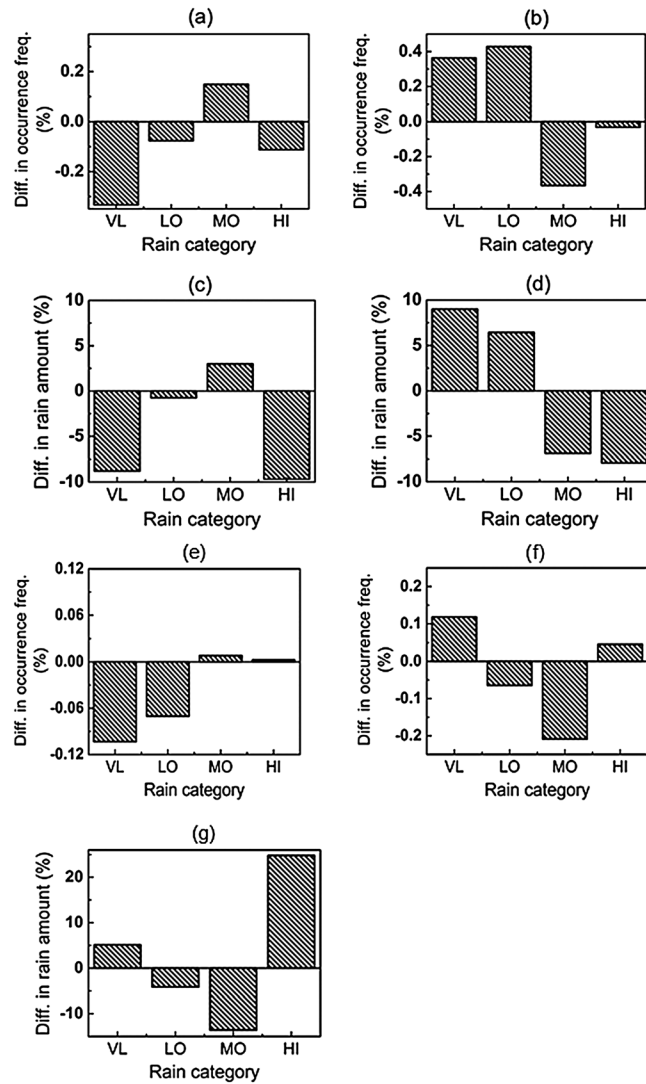


Figure 11. Differences in (a and b) rain occurrence frequency and (c and d) rain amount between polluted and clean simulations for the four precipitation categories over mountain (Figures 11a and 11c) and plain areas (Figures 11b and 11d). For a given rain category over mountain/plain areas, the sum of grid points with a precipitation rate falling in the category divided by the total number of mountain/plain grid points over the 3 days of simulation after the first 6 h spin-up is calculated, then multiplied by 100 to get a percentage. The values shown in Figures 11a and 11b are the differences in rain occurrence frequency between polluted and clean conditions. The rain amount differences in Figures 11c and 11d are calculated as $(\text{Polluted} - \text{Clean}) / \text{Clean} * 100$ for each rain category. (e) The difference of rain occurrence frequency is calculated over mountain during 03:00–09:00 UTC on 13 July for shallow cumulus clouds. Results of (f) rain occurrence frequency and (g) rain amount are from the simulation without terrains.

grid points during the 3 days of simulation after the first 6 h spin-up is calculated. Figure 11 shows differences in the frequency of rain occurrence and rain amount for different rain categories over the mountainous and plain areas. The frequencies of both VL and LO precipitation decrease with increasing aerosols over the mountainous region (Figure 11a) but increase over the plain area (Figure 11b). This agrees with results from the above observational analysis. However, the decreased occurrence frequency of heavy rain under the polluted condition over plain (Figure 11b) is opposite to that from long-term observations (Table 2). This is likely due to the choice of case study carried out here that may not reflect the long-term trend in heavy precipitation

Wind shear is a key factor dictating aerosol-cloud-precipitation interactions for convective clouds. We analyzed the long-term variation in the wind speed trend at various pressure levels in both U and V directions (Figure 10). Wind shear is calculated as $\max(U) / \max(V)$ minus $\min(U) / \min(V)$ within 5 km from ground in the U/V directions. Wind shear at Taihang has a mean value of 8.08 m/s and 2.74 m/s in the U and V wind directions, respectively. Values in the plain area are similar, i.e., 8.19 m/s and 2.52 m/s for U and V wind directions, respectively. There is little difference in the trend in wind shear for mountainous and plain areas. As such, the opposite trends in light rain observed between the two regions (Figure 3) are likely not linked to changes in wind shear.

3.5. Model Results

During the 3 day simulation, clouds over Taihang are mainly mixed-phase stratiform clouds with cloud depths of ~2–5 km. These clouds are much shallower than clouds over the plain area, which are mainly deep clouds. We use the same classification of rainfall intensity as the observational analysis in the modeling analysis. Mountainous and plain areas are defined as grid points with altitudes > 300 m and $10 \text{ m} < \text{altitude} < 100 \text{ m}$ in Domain 2 after excluding the boundary points (Figure 3), respectively. The total numbers of rainy grid points for the 3 day simulation are 604,543 and 605,619 under clean and polluted conditions, respectively, which are sufficient for statistical analysis.

For a given rain category over mountainous/plain areas, the sum of grid points with a precipitation rate falling in the category divided by the total number of mountainous/plain

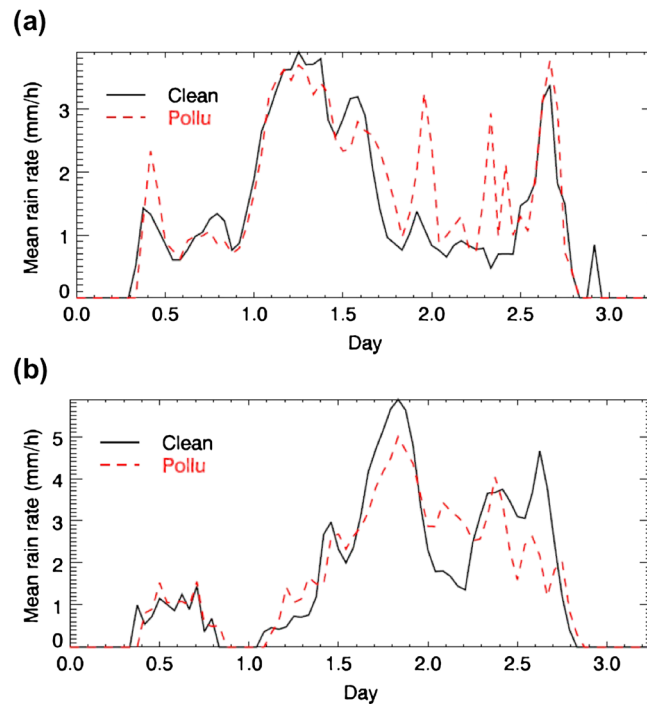


Figure 12. Time evolution of mean rain rate under polluted (red-dashed lines) and clean (black solid lines) conditions for (a) mountain and (b) plain areas. The mean rain rate is averaged over the grid points with rain rates no less than 0.25 mm/h, which is the detection limit of a rain gauge.

rates increased under polluted conditions during most of the simulation period (Figure 12a). This increase is mainly from the moderate precipitation type. Orographic enhancement along the windward slope may explain this feature. For the plain area, mean rain rates under polluted conditions appear to decrease during the simulation period (Figure 12b). This is likely due to the significant reduction of moderate and heavy rain (Figures 11b and 11d).

We also performed sensitivity simulations in which all terrains are removed in the WRF model to investigate the orographic influences separately. Figures 11f and 11g show that without mountains, the occurrence, frequency, and amount of VL/MO rain rate types increase/decrease from the clean to polluted conditions. This is opposite to what is seen in the simulations for the mountainous area, which are shown in Figures 11a and 11c. Therefore, the orographic influence is likely a key factor contributing to the opposite trend in light rain seen in the mountainous and plain area.

Based on the simulations, clouds over the mountainous area are much shallower than those over the plains. Aerosols presumably suppress warm-rain processes, leading to a longer cloud lifetime and reduced light rain for warm and stratiform clouds. For some deep clouds, the delay of early rain by aerosols can result in very heavy rain later on. The increase in MO precipitation events suggests that aerosols may shift precipitation rates from light to moderate. This phenomenon has also been verified by previous observational [Rosenfeld *et al.*, 2008a; Li *et al.*, 2011a] and model studies [Tao *et al.*, 2007]. The change in light rain over the plain area is opposite to that over Taihang; heavy rain increases over both areas. In plain regions where many urban cities are located, the impact of aerosols also depends on factors such as the heat island effect, aerosol type, surface roughness, cloud systems, etc., which deserve more investigation.

The cloud-resolving model results demonstrate that the occurrence frequencies of VL and LO precipitation types decrease significantly over mountainous areas due to aerosol indirect effects, i.e., increasing cloud droplet number concentrations and reducing droplet sizes which suppresses warm-rain processes that produce light rain.

Several previous modeling studies [Wu *et al.*, 2013; Zhang *et al.*, 2012] have suggested that light-absorbing aerosols can have a cooling effect on the surface. This, in turn, modulates the thermodynamical stability of

with aerosols. The main clouds are MSS in our 3 day simulations, but the precipitation during 03:00–09:00 UTC on 13 July (the first day of the simulation) is associated with shallow cumulus clouds (ORO). We examine the responses of ORO separately (Figure 11e) and find that the occurrence frequency of light rain (VL and LO) also decreases from the clean to polluted conditions, consistent with the observational results. The change in rain amount for each rain category from the clean to polluted condition over the mountainous area corresponds well with the change in occurrence frequency (Figures 11a and 11c). For the plain area, the modeled changes in occurrence frequency and rain amount for different precipitation categories from the clean to polluted cases are almost all opposite to those for the mountainous area, particularly for light and moderate precipitation (Figures 11a and 11b). Although the frequency and amount of light rain over the mountainous region decreased due to aerosol indirect effects, mean rain

the atmosphere, changes the atmospheric circulation pattern, and significantly alters the precipitation mechanism in East China, especially during the summer monsoon season. In view of the high BC concentration in northern China [Menon *et al.*, 2002], this could be another possible reason for the observed precipitation variation presented in this study.

4. Conclusions

In a similar manner as in previous studies [Qian *et al.*, 2009] concerning the influence of aerosols on precipitation in this study area, we applied long-term high-resolution (hourly) precipitation data, combined with in situ visibility data, to infer the response of different precipitation mechanisms to aerosol loading, based on observation and modeling.

Forty years (1966–2005) of summertime (May to September) meteorological records, hourly rain gauge data, and daily horizontal visibility records collected at seven weather stations located across the NCP have been examined. The summertime total precipitation in terms of frequency and amount at almost all stations shows no significant trend as visibility decreases over time. However, the frequency of light rain events shows a strong decreasing trend at the mountain stations downwind of the NCP. No clear trend in moderate and heavy rainfall types is seen. Orographic enhancement factors at two pairs of mountain-plain stations (YS/XT and YQ/SJZ) decreased by 25% and 9%, respectively. This may be due to the forced uplifting of the polluted air mass which gives rise to a greater number of smaller cloud droplets that are unable to coalesce and rain out as they pass over the mountains. The observational analysis of the precipitation efficiency of orographic clouds at mountain stations also indicates a decreasing trend as pollution increases, suggesting the role of aerosols in inhibiting light rain.

Considering the various possible influence of aerosol on light rain, we investigated the light rain variation trends at mountainous stations in terms of formation mechanisms of light rain. Both orographic (ORO) rain and large-scale system-induced (MSS) light rain have decreasing trends during the study period except that the ORO mechanism has a relatively lower frequency value when compared with the MSS mechanism. Therefore, light rain at Taihang is likely suppressed due to the aerosol pollution in the NCP, irrespective of the light rain formation mechanisms involved. The increasing trend in atmospheric moisture content, CAPE, and the consistent decreasing trend in wind shear over both mountainous and plain regions are excluded as potential causes.

High-resolution model simulations using clean and polluted conditions indicate that aerosols, by serving as CCN only, contribute significantly to the observed decreases in light rain frequency and amount over the mountainous area. No consistent trend is seen in simulation results for moderate and heavy rainfall types, which is similar to the observational results. Sensitivity simulations in which terrain is removed show an increase in light rain frequency from clean to polluted conditions, opposite to those in simulations with terrain. This suggests that the orographic influence is likely a significant factor contributing to the opposite trends in light rain seen in mountainous and plain areas.

Overall, both observational evidence and modeling tests indicate that aerosol pollution from upwind plain areas could play a significant role in the reduction of light rain observed over the past few decades over mountainous areas. Other factors, such as the urban heat island effect and mechanical convection caused by moisture and roughness, could play important roles in modulating downwind precipitation amounts. Since many cities are located in the NCP, the urban heat island effect is another factor to be considered for precipitation over the plain regions. A better understanding of the link between air pollution and precipitation requires further investigation into issues such as aerosol radiative effects, especially for black carbon/soot aerosols, which lead to low-level wind changes [Alpert *et al.*, 2009; Alpert and Shafir, 1991]. Both aerosol radiative effects and the urban heat island effect will be considered in future modeling work to more exclusively examine aerosol impacts on precipitation.

References

- Albrecht, B. A. (1989), Aerosols, cloud microphysics, and fractional cloudiness, *Science*, 245(4923), 1227–1230.
- Alpert, P., and H. Shafir (1991), On the role of the wind vector interaction with high-resolution topography in orographic rainfall modeling, *Q. J. R. Meteorol. Soc.*, 117(498), 421–426.
- Alpert, P., N. Halfon, and Z. Levin (2008), Does air pollution really suppress precipitation in Israel?, *J. Appl. Meteorol. Climatol.*, 47(4), 933–943, doi:10.1175/2007jamc1803.1.

Acknowledgments

This study was financially supported by the Ministry of Science and Technology of China (grants 2011CB403401, 2013CB955804, and GYHY201206040), the National Natural Science Foundation of China (grant 41171294/41175080), and the Chinese Academy of Meteorological Sciences (grant 2011Y002/2013Z007). We would like to thank National Meteorological Information Center of Chinese Meteorological Administration for providing hourly gauge-based precipitation data. Jiwen Fan and Qian Chen are grateful for the support of the U.S. Department of Energy (DOE) Office of Science Biological and Environmental Research as part of Atmospheric System Research Program. The Battelle Memorial Institute operates the Pacific Northwest National Laboratory for the DOE under contract DE-AC06-76RLO1830. We appreciate very much the valuable comments from three anonymous reviewers, which helped us improve this paper considerably.

- Alpert, P., N. Halfon, and Z. Levin (2009), Comments on "Does air pollution really suppress precipitation in Israel?" Reply, *J. Appl. Meteorol. Climatol.*, *48*(8), 1751–1754, doi:10.1175/2009jamc1943.1.
- Carrió, G. G., W. R. Cotton, and W. Y. Y. Cheng (2010), Urban growth and aerosol effects on convection over Houston: Part I: The August 2000 case, *Atmos. Res.*, *96*(4), 560–574, doi:10.1016/j.atmosres.2010.01.005.
- Che, H., X. Zhang, Y. Li, Z. Zhou, and J. J. Qu (2007), Horizontal visibility trends in China 1981–2005, *Geophys. Res. Lett.*, *34*, L24706, doi:10.1029/2007GL031450.
- Dee, D. P., et al. (2011), The ERA-Interim reanalysis: Configuration and performance of the data assimilation system, *Q. J. R. Meteorol. Soc.*, *137*(656), 553–597, doi:10.1002/qj.828.
- Fan, J., T. Yuan, J. M. Comstock, S. Ghan, A. Khain, L. R. Leung, Z. Li, V. J. Martins, and M. Ovchinnikov (2009), Dominant role by vertical wind shear in regulating aerosol effects on deep convective clouds, *J. Geophys. Res.*, *114*, D22206, doi:10.1029/2009JD012352.
- Fan, J., L. R. Leung, Z. Li, H. Morrison, H. Chen, Y. Zhou, Y. Qian, and Y. Wang (2012a), Aerosol impacts on clouds and precipitation in eastern China: Results from bin and bulk microphysics, *J. Geophys. Res.*, *117*, D00K36, doi:10.1029/2011JD016537.
- Fan, J., D. Rosenfeld, Y. Ding, L. R. Leung, and Z. Li (2012b), Potential aerosol indirect effects on atmospheric circulation and radiative forcing through deep convection, *Geophys. Res. Lett.*, *39*, L09806, doi:10.1029/2012GL051851.
- Fan, J., et al. (2013), Aerosol impacts on California winter clouds and precipitation during CalWater 2011: Local pollution vs. long-range transported dust, *Atmos. Chem. Phys. Discuss.*, *13*(7), 19,921–19,970, doi:10.5194/acpd-13-19921-2013.
- Feingold, G., H. L. Jiang, and J. Y. Harrington (2005), On smoke suppression of clouds in Amazonia, *Geophys. Res. Lett.*, *32*, L02804, doi:10.1029/2004GL021369.
- Givati, A., and D. Rosenfeld (2004), Quantifying precipitation suppression due to air pollution, *J. Appl. Meteorol.*, *43*(7), 1038–1056, doi:10.1175/1520-0450(2004)043<1038:qpsdta>2.0.co;2.
- Goldreich, Y. (2003), *The Climate of Israel: Observation, Research and Application*, Kluwer Academic/Plenum Publishers, New York.
- Gong, D.-Y., C.-H. Ho, D. Chen, Y. Qian, Y.-S. Choi, and J. Kim (2007), Weekly cycle of aerosol-meteorology interaction over China, *J. Geophys. Res.*, *112*, D22202, doi:10.1029/2007JD008888.
- Goswami, B. N., V. Venugopal, D. Sengupta, M. S. Madhusoodanan, and P. K. Xavier (2006), Increasing trend of extreme rain events over India in a warming environment, *Science*, *314*(5804), 1442–1445, doi:10.1126/science.1132027.
- Guo, J., X. Y. Zhang, Y. R. Wu, Y. Zhaxi, H. Z. Che, B. La, W. Wang, and X. W. Li (2011), Spatio-temporal variation trends of satellite-based aerosol optical depth in China during 1980–2008, *Atmos. Environ.*, *45*(37), 6802–6811, doi:10.1016/j.atmosenv.2011.03.068.
- Guo, J., P. Zhai, L. Wu, M. Cribb, Z. Li, Z. Ma, F. Wang, D. Chu, P. Wang, and J. Zhang (2014), Diurnal variation and the influential factors of precipitation from surface and satellite measurements in Tibet, *Int. J. Climatol.*, doi:10.1002/joc.3886.
- Halfon, N., Z. Levin, and P. Alpert (2009), Temporal rainfall fluctuations in Israel and their possible link to urban and air pollution effects, *Environ. Res. Lett.*, *4*, 025001, doi:10.1088/1748-9326/4/2/025001.
- Hand, J., S. Kreidenweis, D. Eli Sherman, J. Collett, S. Hering, D. Day, and W. Malm (2002), Aerosol size distributions and visibility estimates during the Big Bend regional aerosol and visibility observational (BRAVO) study, *Atmos. Environ.*, *36*(32), 5043–5055, doi:10.1016/S1352-2310(02)00568-X.
- Houze, R. A. J. (2012), Orographic effects on precipitation clouds, *Rev. Geophys.*, *50*, RG1001, doi:10.1029/2011RG000365.
- Jiang, J. H., H. Su, M. R. Schoeberl, S. T. Massie, P. Colarco, S. Platnick, and N. J. Livesey (2008), Clean and polluted clouds: Relationships among pollution, ice clouds, and precipitation in South America, *Geophys. Res. Lett.*, *35*, L14804, doi:10.1029/2008GL034631.
- Khain, A. P. (2009), Notes on state-of-the-art investigations of aerosol effects on precipitation: A critical review, *Environ. Res. Lett.*, *4*(1), 015004, doi:10.1088/1748-9326/4/1/015004.
- Khain, A., A. Pokrovsky, M. Pinsky, A. Seifert, and V. Phillips (2004), Simulation of effects of atmospheric aerosols on deep turbulent convective clouds using a spectral microphysics mixed-phase cumulus cloud model. Part I: Model description and possible applications, *J. Atmos. Sci.*, *61*(24), 2963–2982, doi:10.1175/jas-3350.1.
- Khain, A. P., A. Pokrovsky, U. Blahak, and D. Rosenfeld (2008), Is the dependence of warm and ice precipitation on the aerosol concentration monotonic, paper presented at Extended Abstract for the 15th International Conference on Clouds and Precipitation, Cancun, Mexico.
- Khain, A. P., B. Lynn, and J. Dudhia (2010), Aerosol effects on intensity of landfalling hurricanes as seen from simulations with the WRF model with spectral bin microphysics, *J. Atmos. Sci.*, *67*(2), 365–384, doi:10.1175/2009JAS3210.1.
- Koren, I., J. V. Martins, L. A. Remer, and H. Afargan (2008), Smoke invigoration versus inhibition of clouds over the Amazon, *Science*, *321*(5891), 946–949, doi:10.1126/science.1159185.
- Koren, I., O. Altaratz, L. A. Remer, G. Feingold, J. V. Martins, and R. H. Heiblum (2012), Aerosol-induced intensification of rain from the tropics to the mid-latitudes, *Nat. Geosci.*, *5*, 118–122, doi:10.1038/ngeo1364.
- Lee, K.-H., Z. Li, M.-S. Wong, J. Xin, W.-M. Hao, and F. Zhao (2007), Aerosol single scattering albedo estimated across China from a combination of ground and satellite measurements, *J. Geophys. Res.*, *112*, D22S15, doi:10.1029/2007JD009077.
- Li, C., J. W. Stehr, L. T. Marufu, Z. Li, and R. R. Dickerson (2012), Aircraft measurements of SO₂ and aerosols over northeastern China: Vertical profiles and the influence of weather on air quality, *Atmos. Environ.*, *62*, 492–501, doi:10.1016/j.atmosenv.2012.07.076.
- Li, Z., et al. (2007), Preface to special section on East Asian Studies of Tropospheric Aerosols: An International Regional Experiment (EAST-AIRE), *J. Geophys. Res.*, *112*, D22S00, doi:10.1029/2007JD008853.
- Li, Z., F. Niu, J. Fan, Y. Liu, D. Rosenfeld, and Y. Ding (2011a), Long-term impacts of aerosols on the vertical development of clouds and precipitation, *Nat. Geosci.*, *4*(12), 888–894, doi:10.1038/ngeo1313.
- Li, Z., et al. (2011b), East Asian Studies of Tropospheric Aerosols and their Impact on Regional Climate (EAST-AIRC): An overview, *J. Geophys. Res.*, *116*, D00K34, doi:10.1029/2010JD015257.
- Lin, J. C., T. Matsui, R. A. Pielke, Sr., and C. Kummerow (2006), Effects of biomass-burning-derived aerosols on precipitation and clouds in the Amazon Basin: A satellite-based empirical study, *J. Geophys. Res.*, *111*, D19204, doi:10.1029/2005JD006884.
- Menon, S., J. Hansen, L. Nazarenko, and Y. Luo (2002), Climate effects of black carbon aerosols in China and India, *Science*, *297*(5590), 2250–2253.
- Niemand, M., et al. (2012), A particle-surface-area-based parameterization of immersion freezing on desert dust particles, *J. Atmos. Sci.*, *69*(10), 3077–3092, doi:10.1175/jas-d-11-0249.1.
- Paldor, N. (2008), On the estimation of trends in annual rainfall using paired gauge observations, *J. Appl. Meteorol. Climatol.*, *47*(6), 1814–1818, doi:10.1175/2007JAMC1697.1.
- Qian, Y., D. P. Kaiser, L. R. Leung, and M. Xu (2006), More frequent cloud-free sky and less surface solar radiation in China from 1955 to 2000, *Geophys. Res. Lett.*, *33*, L01812, doi:10.1029/2005GL024586.
- Qian, Y., D. Y. Gong, J. W. Fan, L. R. Leung, R. Bennartz, D. L. Chen, and W. G. Wang (2009), Heavy pollution suppresses light rain in China: Observations and modeling, *J. Geophys. Res.*, *114*, D00K02, doi:10.1029/2008JD011575.

- Rosenfeld, D. (1999), TRMM observed first direct evidence of smoke from forest fires inhibiting rainfall, *Geophys. Res. Lett.*, *26*(20), 3105–3108, doi:10.1029/1999GL006066.
- Rosenfeld, D., J. Dai, X. Yu, Z. Yao, X. Xu, X. Yang, and C. Du (2007), Inverse relations between amounts of air pollution and orographic precipitation, *Science*, *315*(5817), 1396–1398, doi:10.1126/science.1137949.
- Rosenfeld, D., U. Lohmann, G. B. Raga, C. D. O'Dowd, M. Kulmala, S. Fuzzi, A. Reissell, and M. O. Andreae (2008a), Flood or drought: How do aerosols affect precipitation?, *Science*, *321*(5894), 1309–1313, doi:10.1126/science.1160606.
- Rosenfeld, D., W. L. Woodley, D. Axisa, E. Freud, J. G. Hudson, and A. Givati (2008b), Aircraft measurements of the impacts of pollution aerosols on clouds and precipitation over the Sierra Nevada, *J. Geophys. Res.*, *113*, D15203, doi:10.1029/2007JD009544.
- Russell, A., and M. Hughes (2012), Is the changing precipitation regime of Manchester, United Kingdom, driven by the development of urban areas?, *Int. J. Climatol.*, *32*(6), 974, doi:10.1002/joc.2321.
- Stevens, B., and G. Feingold (2009), Untangling aerosol effects on clouds and precipitation in a buffered system, *Nature*, *461*(7264), 607–613, doi:10.1038/nature08281.
- Sumner, G. N. (1988), *Precipitation: Process and Analysis*, John Wiley, New York.
- Tao, W. K., X. Li, A. Khain, T. Matsui, S. Lang, and J. Simpson (2007), Role of atmospheric aerosol concentration on deep convective precipitation: Cloud-resolving model simulations, *J. Geophys. Res.*, *112*, D24518, doi:10.1029/2007JD008728.
- Tao, W. K., J. P. Chen, Z. Q. Li, C. Wang, and C. D. Zhang (2012), Impact of aerosols on convective clouds and precipitation, *Rev. Geophys.*, *50*, RG2001, doi:10.1029/2011RG000369.
- Twomey, S. (1977), The influence of pollution on the shortwave albedo of clouds, *J. Atmos. Sci.*, *34*(7), 1149–1152, doi:10.1175/1520-0469(1977)034<1149:tiopot>2.0.co;2.
- van den Heever, S. C., and W. R. Cotton (2007), Urban aerosol impacts on downwind convective storms, *J. Appl. Meteorol. Climatol.*, *46*(6), 828–850, doi:10.1175/JAM2492.1.
- Wang, Y., Q. Wan, W. Meng, F. Liao, H. Tan, and R. Zhang (2011), Long-term impacts of aerosols on precipitation and lightning over the Pearl River Delta megacity area in China, *Atmos. Chem. Phys.*, *11*(23), 12,421–12,436.
- Wang, Y., A. Khalizov, M. Levy, and R. Zhang (2013), New directions: Light absorbing aerosols and their atmospheric impacts, *Atmos. Environ.*, *81*, 713–715, doi:10.1016/j.atmosenv.2013.09.034.
- Wu, L., H. Su, and J. H. Jiang (2013), Regional simulation of aerosol impacts on precipitation during the East Asian summer monsoon, *J. Geophys. Res. Atmos.*, *118*, 6454–6467, doi:10.1002/jgrd.50527.
- Xin, J. Y., et al. (2007), Aerosol optical depth (AOD) and Angstrom exponent of aerosols observed by the Chinese Sun Hazemeter Network from August 2004 to September 2005, *J. Geophys. Res.*, *112*, D05203, doi:10.1029/2006JD007075.
- Yang, X., and Z. Li (2014), Increases in thunderstorm activity and relationships with air pollution in Southeast China, *J. Geophys. Res. Atmos.*, *119*, 1835–1844, doi:10.1002/2013JD021224.
- Yang, X., M. Ferrat, and Z. Li (2013a), New evidence of orographic precipitation suppression by aerosols in central China, *Meteorol. Atmos. Phys.*, *119*, 17–29, doi:10.1007/s00703-012-0221-9.
- Yang, X., Z. Yao, Z. Li, and T. Fan (2013b), Heavy air pollution suppresses summer thunderstorms in central China, *J. Atmos. Sol. Terr. Phys.*, *95–96*, 28–40.
- Yu, R., Y. Xu, T. Zhou, and J. Li (2007), Relation between rainfall duration and diurnal variation in the warm season precipitation over central eastern China, *Geophys. Res. Lett.*, *34*, L13703, doi:10.1029/2007GL030315.
- Yum, S. S., and J. W. Cha (2010), Suppression of very low intensity precipitation in Korea, *Atmos. Res.*, *98*(1), 118–124, doi:10.1016/j.atmosres.2010.06.006.
- Zhai, P. M., and R. E. Eskridge (1997), Atmospheric water vapor over China, *J. Clim.*, *10*(10), 2643–2652, doi:10.1175/1520-0442(1997)010<2643:awvoc>2.0.co;2.
- Zhai, P. M., X. Zhang, H. Wan, and X. Pan (2005), Trends in total precipitation and frequency of daily precipitation extremes over China, *J. Clim.*, *18*(7), 1096–1108, doi:10.1175/JCLI-3318.1.
- Zhang, H., Z. Wang, Z. Wang, Q. Liu, S. Gong, X. Zhang, Z. Shen, P. Lu, X. Wei, and H. Che (2012), Simulation of direct radiative forcing of aerosols and their effects on East Asian climate using an interactive AGCM-aerosol coupled system, *Clim. Dyn.*, *38*(7–8), 1675–1693.
- Zhang, R., G. Li, J. Fan, D. L. Wu, and M. J. Molina (2007), Intensification of Pacific storm track linked to Asian pollution, *Proc. Natl. Acad. Sci. U.S.A.*, *104*(13), 5295–5299, doi:10.1073/pnas.0700618104.